Self-Packaged mm-Wave Broadband Air-Filled SIW Filtering Power Divider With Sharp Roll-Off Skirt and High In-Band Isolation

Daotong Li, *Senior Member, IEEE*, Jiaxin Wang, Linsong Shi, Ying Liu, Kai-Da Xu, *Senior Member, IEEE*, Qiang Chen, *Senior Member, IEEE*, and Naoki Shinohara, *Senior Member, IEEE*

***Abstract*— A self-packaged air-filled substrate-integrated waveguide (AFSIW) filtering power divider (FPD) operating at *Ka*-band with the characteristics of low loss, broadband, high in-band isolation, and sharp roll-off skirt is proposed in this letter. The filtering network is dexterously integrated into the branches of the T-junction, which is simple and compact. It is investigated in a 1-2way modified T-junction with integrated absorbers, which exhibits broadband and high in-band isolation characteristics. Cross-coupling technology is used to further improve frequency selectivity by introducing controllable transmission zeros (TZs). The prototype of FPD with a center frequency of 31.3 GHz, a −3-dB fractional bandwidth (FBW) of 16.8%, an insertion loss (IL) of 3.9 dB, a return loss (RL) of more than 18.2 dB, an in-band isolation ($|S_{23}|$) of not less than 17.6 dB, and an out-of-band suppression of more than 24 dB is designed, fabricated, and measured. The measured and simulated results agree well.**

***Index Terms*— Air-filled substrate-integrated waveguide (AFSIW), broadband, filtering power divider (FPD), integrated filtering network, low loss, T-junction.**

I. Introduction

THE rapid development of millimeter-wave (mm-wave) communication has put forward higher demands on radio frequency (RF) components [1]. Filtering power dividers (FPDs), as multifunctional passive components for power distribution and signal selection, play a key role in communication systems [2]. Therefore, it is of great application importance to study high performance and compact FPDs suitable for mm-wave communication.

Reviewing the literature, some microstrip FPDs based on single-layer printed circuit board (PCB) technology and low-temperature co-fired ceramic (LTCC) technology [3], [4], [5] excel in miniaturization due to their compactness. However, microstrip-based components suffer from severe losses, which worsen with increasing frequency. Due to the advantages of low loss and high Q value, substrate-integrated waveguide (SIW) has attracted a lot of interest in the past two decades [6], [7]. To the best of our knowledge, the SIW-based design of FPDs is mainly achieved by cascading multiple SIW resonant cavities coupled to achieve the filter response [8], [9], [10], but it will increase additional sizes. In [10], a single-layer dual-band SIW FPD based on three SIW cavities with fully differential operation at 28 and 39 GHz is proposed; however, the average insertion loss (IL) in the passbands reaches 4.7 and 5.2 dB, respectively. It is due to the fact that the dielectric loss of SIW accounts for most of its total transmission loss in the mm-wave band [11]. Recently, air-filled SIW (AFSIW) based on multilayer PCB technology provides a new scheme for mm-wave circuits design [12], which has lower loss, higher power handling capacity performance, and self-packaged performance than SIW. Since then, various RF components have been proposed using AFSIW technology, such as filters [13], power dividers/combiners [14], [15], couplers [16], FPDs [17], and so on. In [17], a low-loss AFSIW FPD operating at 5.5 GHz is proposed, which reduces the size by directly connecting coaxial lines to AFSIW cavities, but it results in severe energy crosstalk between the output ports and poor isolation performance in the passband.

In this letter, a novel low-loss self-packaged FPD in the Ka-band based on AFSIW platform is presented. The strategy of dexterously integrating the filtering network into the branches of the T-junction is investigated in a 1-2way T-junction. A modified T-junction and absorbers integration topology is utilized to realize high in-band isolation performance. To further improve the frequency selectivity, transmission zeros (TZs) are introduced based on cross-coupling technology, which is controllable by adjusting the size of coupling slots. The proposed FPD is compact and suitable for mm-wave circuits and systems with high-performance requirements.

Manuscript received 27 January 2024; revised 7 March 2024; accepted 24 March 2024. Date of publication 3 April 2024; date of current version 10 May 2024. This work was supported in part by the National Natural Science Foundation of China under Grant 61801059 and in part by the Basic Research and Frontier Exploration Special of Chongqing Natural Science Foundation under Grant cstc2019jcyj-msxmX0350. *(Corresponding author: Daotong Li.)*

Daotong Li is with the School of Microelectronics and Communication Engineering, Chongqing University, Chongqing 400044, China, and also with the Research Institute for Sustainable Humanosphere, Kyoto University, Kyoto 606-8501, Japan (e-mail: dli@cqu.edu.cn).

Jiaxin Wang, Linsong Shi, and Ying Liu are with the School of Microelectronics and Communication Engineering, Chongqing University, Chongqing 400044, China.

Kai-Da Xu is with the School of Information and Communications Engineering, Xi'an Jiaotong University, Xi'an 710049, China.

Qiang Chen is with the Department of Communications Engineering, Tohoku University, Sendai 980-8579, Japan.

Naoki Shinohara is with the Research Institute for Sustainable Humanosphere, Kyoto University, Kyoto 606-8501, Japan.

Color versions of one or more figures in this letter are available at https://doi.org/10.1109/LMWT.2024.3382592.

Digital Object Identifier 10.1109/LMWT.2024.3382592

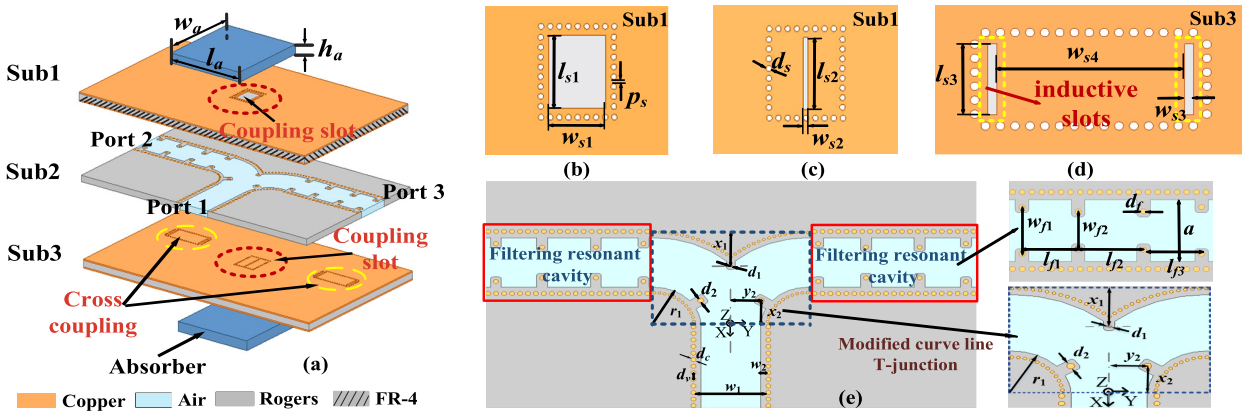

Fig. 1. Structure of the proposed AFSIW FPD. (a) Three-dimensional view, (b) top view of coupling slot on Sub1 and bottom view of coupling slot on Sub3, (c) bottom view of coupling slot on Sub1 and top view of coupling slot on Sub3, (d) cross coupling slot on Sub3, and (e) details of Sub2.

TABLE I

PARAMETERS OF THE PROPOSED AFSIW FPD (UNIT: MM)

w_1=7.04	w_2=0.508	a=6.024	w_a=10	l_a=10	w_{s1}=3.1	l_{s1}=3.7
w_{s2}=0.25	l_{s2}=3.7	d_1=0.3	d_2=0.6	d_f=0.5	r_1=4.8	x_1=4.15
x_2=3.1	y_2=3.042	w_{f1}=4.6	w_{f2}=3.75	l_{f1}=4.65	l_{f2}=5.4	l_{f3}=4.8
w_{s3}=0.25	w_{s4}=6.32	l_{s3}=2.52	d_c=0.5	d_v=0.8	d_s=0.3	P_s=0.2

II. ANALYSIS AND DESIGN OF THE AFSIW FPD

Fig. 1(a) shows the configuration of the proposed FPD, which consists of three layers of substrates. The layer Sub1 is low-cost FR-4 ($h_1 = 0.5$ mm, $\varepsilon_r = 4.4$, and tan $\delta_d = 0.02$). Both the layers Sub2 and Sub3 are RT6002 ($h_2 = h3 = 0.508$ mm, ε_r =2.94, and tan$\delta_d = 0.0012$). The coupling slots on Sub1 and Sub3 are symmetrical, and the details are shown in Fig. 1(b) and (c). Cross-coupling slots are shown in Fig. 1(d). Sub2 is the main circuit layer in the middle, and the details are shown in Fig. 1(e). The material used for the absorbers mounted on Sub1 and Sub3 in this work is Eccosorb GDS rubber absorbing materials with a high $h_a = 0.76$ mm, $\varepsilon_r = 13$, $\mu_r = 1.7$, tan$\delta_d = 0.2$, and tan$\delta_m = 0.78$. The detailed dimensions of the FPD are listed in Table I.

A. Isolated Unit Based on Modified T-Junction and Absorbers

Since the environment of mm-wave communication is relatively complex, FPDs need to be highly isolated and stable in performance. The topology of modified T-junction and absorbers is utilized as a broadband isolated power division unit, as illustrated in Fig. 1(a) and (e). The modified curve line T-junction can reduce the discontinuity of the junction as much as possible [18], and the absorbers are less susceptible to high-frequency parasitic impedance when compared to isolation resistors as demonstrated in [14] and [15]. As can be seen from Fig. 2(a), the isolation of the FPD with the topology of modified T-junction and absorbers is more than 15 dB over the entire working band. Moreover, the low sensitivity to dimensional changes of the absorber is additionally investigated in this letter, as shown in Fig. 2(b) and (c), which is important for reducing errors in practical assembly applications.

B. Analysis and Design of the Integrated Filtering Network

The filtering networks are realized by introducing three pairs of inductive posts, which are symmetrically integrated into the

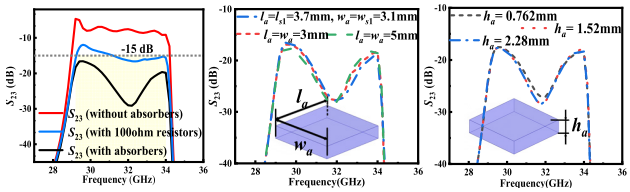

Fig. 2. (a) Simulated S_{23} of FPD with/without absorbers and with 100-Ω resistors. (b) S_{23} versus the length l_a and width w_a of absorbers. (c) S_{23} versus the height h_a of absorbers.

branches, where ports 2 and 3 are located of the T-junction, as shown in Fig. 1(e). The third-order Chebyshev bandpass filtering response can be obtained based on the J–K inverter synthesis design method [19]. The electrical lengths ϕ_i and the physical lengths l_{fi} of the filtering cavity can be calculated by the following formulas [20], [21]:

$$\Delta = \left(\lambda_{g1} - \lambda_{g2}\right)/\lambda_{g0} \tag{1}$$

$$K_{i,i+1} = \left(\frac{\pi\Delta}{2}\left(\frac{\lambda_{g\text{AFSIW}}}{\lambda_0}\right)^2\right)\Big/\sqrt{g_i g_{i+1}} (i = 0, 1, \ldots, n) \tag{2}$$

$$\frac{X_{i,i+1}}{Z_0} = \frac{K_{i,i+1}}{Z_0}\Big/\left(1 - \left(\frac{K_{i,i+1}}{Z_0}\right)^2\right) \tag{3}$$

$$\phi_{i+1} = -\tan^{-1}\left(\frac{2X_{i,i+1}}{Z_0}\right) \ (i = 0, 1, \ldots, n-1) \tag{4}$$

$$l_{fi+1} = \frac{\lambda_{g0}}{2\pi}\left(\pi + \frac{1}{2}(\phi_i + \phi_{i+1})\right)(i = 0, 1, \ldots, n-1) \tag{5}$$

where g_i is an n-order low-pass filter that normalizes the component values (here, $n = 3$, $g_0 = 1$, $g_1 = 2.0236$, $g_2 = 0.9941$, $g_3 = 2.0236$, and $g_4 = 1$), and λ_{g0}, λ_{g1}, and λ_{g2} are the guided wavelengths at the center, lower, and upper frequencies, respectively. Finally, the lengths of the filtering cavity obtained by calculation and optimization in the simulation software are $l_{f1} = 4.65$ mm, $l_{f2} = 5.4$ mm, and $l_{f3} = 4.8$ mm.

Benefited from the multilayer characteristics of AFSIW, a pair of inductive slots is etched on bottom layer (Sub3) to construct cross-coupling multipath, as shown in Fig. 1(d) [22]. The coupling diagram is shown in Fig. 3(a). Paths ①–③ located in Sub 2 are the primary path, and paths ①–③ located in Sub 3 are the secondary path. It can be known that the phase shift of the resonator is −90° above the passband. Considering that AFSIW transmission line will bring an additional

TABLE II
TOTAL PHASE SHIFT OF AFSIW FPD FOR TWO PATHS

Total phase shift	Above resonance
Path I: ①-②-③	-90°-90°-90° = -270°
Path II: ①-③	-90° +Φ_{SIW}
Φ_{SIW} = 360°	Out of phase (with a TZ)

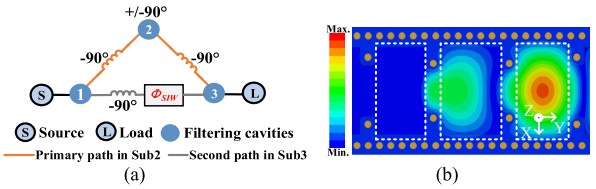

(a) (b)

Fig. 3. (a) Cross-coupling diagram of the proposed FPD and (b) electric field distribution of the transmission path at 34.3 GHz.

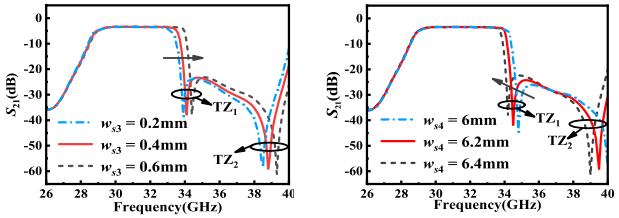

(a) (b)

Fig. 4. Simulated S_{21} variations versus some physical parameters of (a) w_{s3} and (b) w_{s4}, respectively.

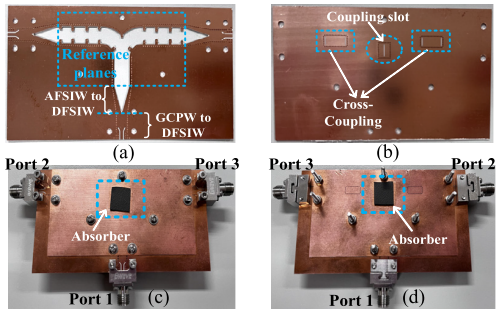

(a) (b) (c) (d)

Fig. 5. Fabrication of AFSIW FPD. (a) Layer Sub2, (b) layer Sub3, (c) top view of the whole structure, and (d) bottom view of the whole structure.

phase Φ_{SIW}, hence, the electrical length of the cross-coupling transmission path is designed to be λ. The details of the phase shifts are shown in Table II. As shown in Fig. 3(b), the E-field distribution is almost attenuated to zero, which corresponds to the theoretically constructed TZ at 34.3 GHz.

Since the size of the cross-coupling slots and the length of the AFSIW transmission line are the key factors affecting the TZs, the impacts of parameters w_{s3} and w_{s4} on the transmission coefficients are investigated. As illustrated in Fig. 4(a) and (b), the position of the TZs and the out-of-band suppression performance can be adjusted by tuning w_{s3} and w_{s4}. Thus, the bandwidth and stopband performance of the proposed AFSIW FPD can be adjusted flexibly.

III. MANUFACTURING, PACKAGING, AND EXPERIMENTAL RESULTS

The prototype of the proposed AFSIW FPD is fabricated based on the standard PCB process, as shown in Fig. 5, and the physical size of the FPD is $4.27\lambda_g \times 8.24\lambda_g \times 0.15\lambda_g$. To achieve the effective interconnection of the air-dielectric-filled SIW circuits, the asymptotic transition is applied to improve the return loss (RL). The measured and simulated results are shown in Fig. 6(a)–(c). It can be seen from Fig. 6(a) that the working frequency band of the proposed AFSIW FPD

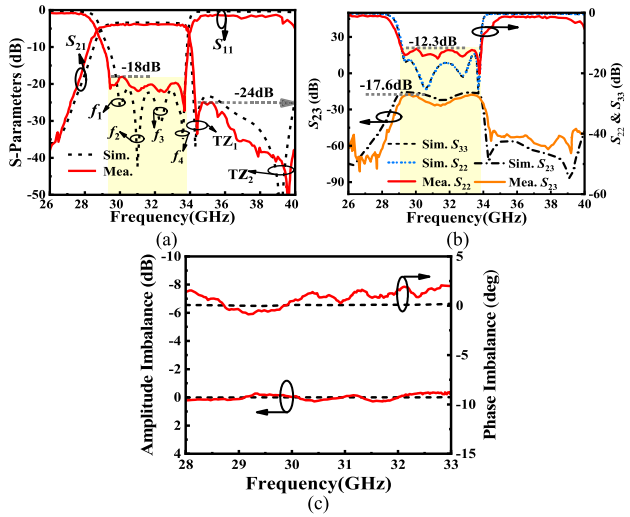

(a) (b) (c)

Fig. 6. Comparison of the measured and simulated results. (a) S_{11}/S_{21}, (b) S_{23}/S_{22}, and (c) amplitude imbalance and phase imbalance.

TABLE III
COMPARISON WITH OTHER PREVIOUS WORKS

Ref.	Technology/ f_0 (GHz)	*IL* (dB)	*RL* (dB)	$\lvert S_{23}\rvert$ (dB)	FBW (%)	TZ	OS (dB)	F.R.
[3]	LTCC/5.5	<5.1	>10	>15	10.5	0	>15	Yes
[6]	SIW/11.8	<3.8	>19.6	>16	5.9	1	>15	Yes
[10]	SIW/28 and 39 (dual band)	<4.7/ <5.2	>14.1/ >14.2	>20/ >14.9	3.2/ 3.1	3	>20	Yes
[15]	AFSIW/33.5	<4.1	>12	>10	33.8	N.A.	N.A.	No
[17]	AFSIW/ 5.45	>4	>11	N.A.	11.2	0	>20	Yes
This work	**AFSIW/ 31.3**	**<3.9**	**>18.2**	**>17.6**	**16.8**	**2**	**>24**	**Yes**

FBW: 3-dB fractional bandwidth, F.R.: Filter Response, OS: out-of-band suppression (upper stopband), N.A.: the data are not available in the reference.

ranges from 28.67 to 33.92 GHz, with the center frequency f_0 of 31.3 GHz at the *Ka*-band and −3-dB FBW of 16.8%. The in-band RL is better than 18.2 dB, the IL is less than 3.9 dB, and the out-of-band suppression is better than 24 dB with two TZs ranging from 34.4 to 39.6 GHz. The measured S_{22} is better than −12.3 dB, as shown in Fig. 6(b), while the in-band isolation S_{23} is greater than −17.6 dB. Moreover, Fig. 6(c) plots the amplitude and phase differences of the FPD, and the proposed FPD has an amplitude imbalance of no more than 0.3 dB and a phase imbalance of no more than 2.3°. The measured results agree well with the simulated ones. The inconsistencies between the simulated and measured results may be caused by fabricating accuracy error and experimental assembly errors.

Moreover, the comparison of the proposed work with some typical letters, as shown in Table III, when the frequency rises up to mm-wave band, the proposed self-packaged AFSIW FPD has the advantages of low loss, high isolation, broadband, and deep out-of-band suppression performance.

IV. CONCLUSION

In this study, an AFSIW FPD with a simple and compact structure operating in the *Ka*-band is realized by integrating the filtering network into the branches of the T-junction. This integration strategy offers significant advantages over the conventional approach of directly cascading filters and power dividers, as it reduces the additional sizes and losses. High isolation characteristic is obtained based on the topology of the modified T-junction and absorbers. Cross-coupling technology is also applied to further enhance the frequency selectivity.

REFERENCES

[1] B. A. Belyaev, A. M. Serzhantov, Y. F. Bal'va, R. G. Galeev, and A. A. Leksikov, "Design for a self-packaged all-PCB wideband filter with good stopband performance," *IEEE Trans. Compon., Packag., Manuf. Technol.*, vol. 12, no. 7, pp. 1186–1195, Jul. 2022.

[2] G. Zhang et al., "Wideband three-way filtering power divider on one single multimode patch resonator," *IEEE Trans. Plasma Sci.*, vol. 50, no. 9, pp. 3270–3275, Sep. 2022.

[3] X. Y. Zhang, X.-F. Liu, Y. C. Li, W.-L. Zhan, Q. Y. Lu, and J.-X. Chen, "LTCC out-of-phase filtering power divider based on multiple broadside coupled lines," *IEEE Trans. Compon., Packag., Manuf. Technol.*, vol. 7, no. 5, pp. 777–785, May 2017.

[4] K. Xu, J. Shi, W. Zhang, and G. M. Mbongo, "The compact balanced filtering power divider with in-phase or out-of-phase output using H-shape resonators," *IEEE Access*, vol. 6, pp. 38490–38497, 2018.

[5] G. Zhang, Z. Qian, J. Yang, and J.-S. Hong, "Wideband four-way filtering power divider with sharp selectivity and high isolation using coshared multi-mode resonators," *IEEE Microw. Wireless Compon. Lett.*, vol. 29, no. 10, pp. 641–644, Oct. 2019.

[6] G. Zhang, Y. Liu, E. Wang, and J. Yang, "Multilayer packaging SIW three-way filtering power divider with adjustable power division," *IEEE Trans. Circuits Syst. II, Exp. Briefs*, vol. 67, no. 12, pp. 3003–3007, Dec. 2020.

[7] L. Zhu et al., "A design method to realize manufacture-friendly millimeter-wave folded substrate integrated waveguide bandpass filters," *IEEE Trans. Circuits Syst. II, Exp. Briefs*, vol. 70, no. 3, pp. 979–983, Mar. 2023.

[8] Y.-X. Huang, Y.-X. Yan, W. Yu, W. Qin, and J.-X. Chen, "Integration design of millimeter-wave bidirectional endfire filtenna array fed by SIW filtering power divider," *IEEE Antennas Wireless Propag. Lett.*, vol. 21, pp. 1457–1461, 2022.

[9] Y.-X. Yan, W. Yu, and J.-X. Chen, "Millimeter-wave low side- and back-lobe SIW filtenna array fed by novel filtering power divider using hybrid TE101/TE301 mode SIW cavities," *IEEE Access*, vol. 9, pp. 167706–167714, 2021.

[10] P.-L. Chi, Y.-M. Chen, and T. Yang, "Single-layer dual-band balanced substrate-integrated waveguide filtering power divider for 5G millimeter-wave applications," *IEEE Microw. Wireless Compon. Lett.*, vol. 30, no. 6, pp. 585–588, Jun. 2020.

[11] F. Parment, A. Ghiotto, T.-P. Vuong, J.-M. Duchamp, and K. Wu, "Broadband transition from dielectric-filled to air-filled substrate integrated waveguide for low loss and high power handling millimeter-wave substrate integrated circuits," in *IEEE MTT-S Int. Microw. Symp. Dig.*, Tampa, FL, USA, Jun. 2014, pp. 1–3.

[12] F. Parment, A. Ghiotto, T.-P. Vuong, J.-M. Duchamp, and K. Wu, "Air-filled substrate integrated waveguide for low-loss and high power-handling millimeter-wave substrate integrated circuits," *IEEE Trans. Microw. Theory Techn.*, vol. 63, no. 4, pp. 1228–1238, Apr. 2015.

[13] T. Martin, A. Ghiotto, and F. Lotz, "Compact G-CPW fed air-filled SIW (AFSIW) filters for systems on substrate," in *IEEE MTT-S Int. Microw. Symp. Dig.*, Perugia, Italy, Nov. 2021, pp. 59–61.

[14] N.-H. Nguyen, A. Ghiotto, T. Martin, A. Vilcot, T.-P. Vuong, and K. Wu, "AFSIW power divider with isolated outputs based on balanced-delta-port magic-tee topology," in *IEEE MTT-S Int. Microw. Symp. Dig.*, Los Angeles, CA, USA, Aug. 2020, pp. 743–746.

[15] N.-H. Nguyen, A. Ghiotto, T. Martin, A. Vilcot, K. Wu, and T.-P. Vuong, "Fabrication-tolerant broadband air-filled SIW isolated power dividers/combiners," *IEEE Trans. Microw. Theory Techn.*, vol. 69, no. 1, pp. 603–615, Jan. 2021.

[16] A. Ghiotto, J.-C. Henrion, T. Martin, J.-M. Pham, and V. Armengaud, "AFSIW-to-microstrip directional coupler for high-performance systems on substrate," in *IEEE MTT-S Int. Microw. Symp. Dig.*, Los Angeles, CA, USA, Aug. 2020, pp. 173–176.

[17] A. Moznebi, K. Afrooz, and M. Danaeian, "High-performance filtering power divider based on air-filled substrate integrated waveguide technology," *ETRI J.*, vol. 45, no. 2, pp. 338–345, Jul. 2022.

[18] S. H. Shehab, N. C. Karmakar, and J. Walker, "Substrate-integrated-waveguide power dividers: An overview of the current technology," *IEEE Antennas Propag. Mag.*, vol. 62, no. 4, pp. 27–38, Aug. 2020.

[19] H. J. Tang, W. Hong, Z. C. Hao, J. X. Chen, and K. Wu, "Optimal design of compact millimetre-wave SIW circular cavity filters," *Electron. Lett.*, vol. 41, no. 19, p. 1068, 2005.

[20] Y. Su, Y. Fan, X. Q. Lin, and K. Wu, "Single-layer mode composite coplanar waveguide dual-band filter with large frequency ratio," *IEEE Trans. Microw. Theory Techn.*, vol. 68, no. 6, pp. 2320–2330, Jun. 2020.

[21] N. H. Nguyen, F. Parment, A. Ghiotto, K. Wu, and T. P. Vuong, "A fifth-order air-filled SIW filter for future 5G applications," in *IEEE MTT-S Int. Microw. Symp. Dig.*, Pavia, Italy, Sep. 2017, pp. 1–3.

[22] T. Martin, A. Ghiotto, T.-P. Vuong, K. Wu, and F. Lotz, "Compact quasi-elliptic and highly selective AFSIW filter with multilayer cross-coupling," in *IEEE MTT-S Int. Microw. Symp. Dig.*, Boston, MA, USA, Jun. 2019, pp. 718–721.